Theor Chem Acc (2011) 129:131–139
DOI 10.1007/s00214-011-0908-x

REGULAR ARTICLE

Structure and electronic properties of tris(4-hydroxy-1,5-naphthyridinato) aluminum (AlND3) and its methyl derivatives: a theoretical study

J. Laxmikanth Rao · K. Bhanuprakash

Received: 5 August 2010 / Accepted: 10 February 2011 / Published online: 27 February 2011

Abstract Molecular structures of the ground state (S_0) of tris(4-hydroxy-1,5-naphthyridinato) aluminum (AlND3) and its methyl derivatives have been optimized using B3LYP/6-31G(D) and the first singlet excited state (S_1) using CIS/6-31G(D) method, respectively. The frontier molecular orbitals characteristics of these Al-complexes have been analyzed systematically in order to understand the electronic transitions. It is seen from these results that in all these complexes, like in earlier reported *mer*-Alq3, the highest occupied molecular orbital (HOMO) is localized on the pyridine-4-ol ring of A-ligand while lowest unoccupied molecular orbital (LUMO) is on the pyridyl ring of B-ligand for S_0 states irrespective of the methyl substitution present on the ligands. The absorption and emission wavelengths have been evaluated at the TD-PBE0/6-31G(D) level and found to be comparable with the experiment. The charge transfer integrals have been calculated for AlND3, and results reveals that electron transport is larger than hole transport. The reorganization energies have been calculated at B3LYP/6-31G(D) level for these complexes, and the results show that the charge mobilities of these complexes are comparable with *mer*-Alq3.

Keywords OLED · AlND3 · Optical properties · Charge transfer integrals · Reorganization energy

Electronic supplementary material The online version of this article (doi:10.1007/s00214-011-0908-x) contains supplementary material, which is available to authorized users.

J. Laxmikanth Rao (✉) · K. Bhanuprakash
Inorganic and Physical Chemistry Division, Indian Institute of Chemical Technology, Hyderabad 500 007, India
e-mail: lkjoshiji@yahoo.com

1 Introduction

Recent organic material research has focused on the utilization of conjugated polymers [1, 2] or low molecular weight materials [3] in OLED devices. OLEDs are heterojunction devices in which layers of organic transport materials are usually incorporated into devices as amorphous thin solid films [4]. Following the initial report of utilization of tris(8-hydroxyquinolinolato)aluminum (*mer*-Alq3) [5, 6] as electron transport material and emitting layer in OLED, the derivatives of metal quinolates have become the focus of new electroluminescent materials research [7, 8] with *mer*-Alq3 being the most often used [9]. Although research into the development of OLEDs in the past decade is rapidly growing; only in recent years, the studies of the fundamental molecular properties of metaloquinolates have been reported in the literature [10–24]. The majority of the reports deal with the ground-state characteristics of *mer*-Alq3 [10–16] and on vertical excitations studies of *mer*-Alq3 using theoretical methods [17–24]. It is clear from these reports that for a better understanding and to make progress in the improvement of OLED devices, the studies on molecular structure of low-weight organic materials are essential. Hence, the present study deals with the detailed theoretical study of the three Al-complexes for their structural, optical properties namely tris (4-hydroxy-1,5-naphthyridinato) aluminum (AlND3) and its methyl derivatives namely tris(4-hydroxy-8-methyl-1,5-naphthyridinato) aluminum (AlmND3) and tris(4-hydroxy-2,8-dimethyl-1,5-naphthyridinato) aluminum (Almm ND3) that were synthesized by Liao et al. [25] and reported to be the blue version analogs of well-known green fluorophore *mer*-Alq3 and can be used as electron transporting layer as well as emitting layer in the OLEDs. The ground and the first excited singlet-state geometries of these

complexes have been optimized using density functional theory (DFT) and ab initio configuration interaction with single excitations (CIS) method, respectively. The time-dependent DFT (TDDFT) methods have been used to calculate absorption and the emission energies of these complexes, and the results are compared with the available experimental data [25]. The charge transfer integrals have been computed for AlND3, and the reorganization energies for all the complexes have been calculated at B3LYP/6-31G(D) level.

2 Computational methodology

The ground-state geometries of AlND3(**1**) and its methyl derivatives **2** and **3**, depicted in Fig. 1, have been optimized at the B3LYP/6-31G(D) level using G03 package [26], which has been proved to be a reliable approach for *mer*-Alq3 and it derivatives [27–32]. The first excited-state geometries have been optimized using the CIS approach [33]. Earlier, this approach had been successfully applied on *mer*-Alq3 [27, 28] and its nitrogen derivatives [30] as well as other OLED materials [34–38], which has given accurate and reliable results. Hence, in this study, the excited-state optimization has been carried out using the CIS/6-31G(D) method. The absorption spectra and emission spectra have been calculated by PBE0-TDDFT method using B3LYP/6-31G(D)- and CIS/6-31G(D)-optimized geometries, respectively. The charge transfer integrals for AlND3(**1**) have been calculated using the direct coupling method implemented in Q-Chem software [39–43]. The reorganization energies for all the complexes which is one of the important parameter for determining the charge mobilities have been calculated using the B3LYP/6-31G(D) method.

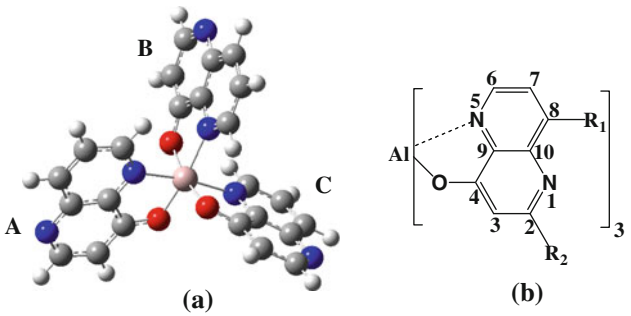

Fig. 1 **a** The geometry of AlND3(**1**) and its methyl derivatives(**2**–**3**) with labels. A–C for three ND ligands. **b** the atom numbering for (**1**–**3**) complexes considered in this work

3 Results and discussions

3.1 Ground-state geometries

The ground-state geometries of the Al-complexes (**1**–**3**) are shown in Fig. 1. The ligands of the complexes (**1**–**3**) have been labeled as A, B, and C. The central Al-atom is surrounded by the three ligands with the A- and C-ligand nitrogens and the B- and C-ligand oxygens *trans* to each other. The selected optimized geometrical parameters of (**1**–**3**) are shown in Table 1, along with the experimental observed parameters for AlND3 [25]. For the sake of comparison, both the optimized geometrical parameters of the *mer*-Alq3 are shown in the same table. It is seen from Table 1 that the calculated average Al–N bond length of **1** (∼2.084 Å) is shorter than that of *mer*-Alq3 (∼2.0913 Å); this could be attributed to the seesaw-like binding mode of the ND ligand [25]. The calculated average Al–O bond length of **1** (∼1.884 Å) is longer than that of *mer*-Alq3 (∼1.873 Å); this may be attributed to the higher electron deficiency of ND ligand compared with 8-hydroxyquinoline, which is evident from their pK_a values [25]. In case of AlND3, the predicted bond lengths of Al–N are 0.059–0.061 Å and for Al–O are 0.005–0.024 Å longer when compared with the experimental data [25]. These bond length and bond angle values compare well with the previously calculated values [29]. The longer predicted bond lengths may partly due to the neglected solid-state effects [44]. Overall, it can be seen that the agreement between the calculated and experimental data is quite good. In case of other complexes namely **2** and **3**, with methyl substitution on the peripheral ligands, negligible increase in the bond length and bond angles is observed when compared with the unsubstituted AlND3.

Table 1 Selected optimized bond lengths in angstrom (A°) and bond angles (deg) for (**1**–**3**) obtained by using the B3LYP/6-31G(D) method

Parameters	1	2	3	Exp[a]	Alq3
Bond lengths					
Al–N_a	2.080	2.076	2.076	2.021	2.084
Al–N_b	2.111	2.103	2.104	2.050	2.126
Al–N_c	2.062	2.056	2.057	2.003	2.064
Al–O_a	1.866	1.869	1.869	1.861	1.855
Al–O_b	1.892	1.894	1.894	1.873	1.881
Al–O_c	1.893	1.895	1.895	1.869	1.884
Bond angles					
Na–Al–Nc	171.72	171.63	171.60	174.21	171.50
Nb–Al–Oa	173.03	172.77	172.88	172.92	172.75
Oc–Al–Ob	167.89	168.03	167.98	171.18	166.57

[a] Experimental data for AlND3(**1**) from [25]

3.2 Frontier molecular orbitals of the ground-state (S_0) geometries

It will be useful to examine the frontier molecular orbitals, i.e., HOMO and LUMOs of these complexes because the relative ordering of these orbitals provides a reasonable qualitative indication of the excitation properties and the ability to electron/hole transport. It can be seen in the literature that in the ground states of *mer*-Alq3 [2, 17, 24] and its nitrogen derivatives [30], the HOMOs are localized mostly on A-ligand while LUMOs are localized on B-ligand. The HOMO, LUMO, and LUMO+1 distribution patterns of (**1**–**3**) in their ground states obtained by using the B3LYP/6-31G(D) method are shown in Fig. 2. In agreement with earlier reports [29, 30], it can be seen that the HOMO and LUMOs of **1** show the similar trend in both the energy values and localization of frontier orbitals at A- and B-ligands, respectively. In all these complexes, the HOMO is localized on the A-ligand and the LUMO is localized on the B-ligand while the LUMOs +1 is mainly localized on C-ligand and to some extent on the A-ligand irrespective of the methyl substitution present on the ligands (Fig. 2). The HOMO, LUMO, and LUMO+1 energies of (**1**–**3**) calculated by TD-PBE0/6-31G(D)//B3LYP/6-31G(D) are tabulated in Table 2. The energy gap (E_{gap}) of (**1**–**3**) have been calculated as the difference of E_{HOMO} and E_{LUMO+1} because in these complexes studied here, the major transitions for the absorptions are from HOMO to LUMO+1 (see details in Table S1). It can be seen that the HOMO, LUMO, and LUMO+1 energy levels of (**1**–**3**) are lower than that of *mer*-Alq3. The energy gaps are found to be ~0.35–0.55 eV higher than the *mer*-Alq3 [45] depending on the substitution, which reflects in their absorption spectra. The difference between the HOMO and LUMO for **1** (0.1508 au) is in good agreement with the previously reported one by B3LYP/DZP method [30].

Table 2 HOMO, LUMO, and energy gaps (E_{gap}) of (**1**–**3**) (in eVs) in their ground state (S_0) obtained by using the TD-PBE0/6-31G(D)//B3LYP/6-31G(D) method

Complexes	HOMO	LUMO	LUMO+1	E_{gap}
Alq3	−5.261	−1.647	−1.405	3.856
1	−6.188	−2.085	−1.843	4.345
2	−6.040	−1.870	−1.638	4.402
3	−5.931	−1.722	−1.492	4.209

3.3 Frontier molecular orbitals of the first excited-state (S_1) geometries

Presently, the standard procedure adopted for calculating the first excited-state equilibrium properties is the CIS

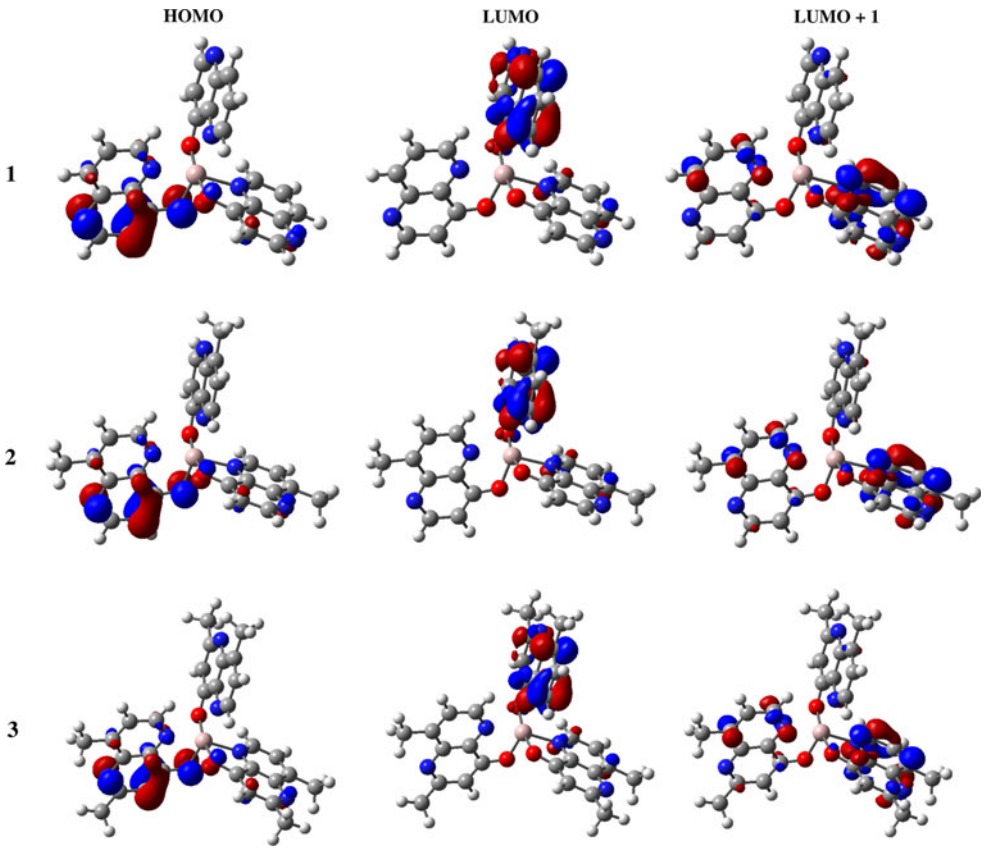

Fig. 2 Frontier molecular orbitals (FMOs) (0.05 e au^{-3}) for the ground states (S_0) of (**1**–**3**)

method [33]. Earlier, this method has been successfully applied on *mer*-Alq3 and its derivatives [27–32] and as well as other OLED materials [34–38]. Hence, the first excited-state geometry optimization for (**1–3**) have been carried out by CIS/6-31G(D) method using the corresponding HF/6-31G(D)-optimized ground-state geometries. The HOMO and LUMO distribution patterns of (**1–3**) in their excited states are shown in Fig. 3. It can be seen from Fig. 3, for the complexes **1** and **2**, the HOMO is localized on the pyridine-4-ol ring of A-ligand while the LUMO is on the pyridyl ring of A-ligand for S_1 sates where as in complex **3**, the HOMO is localized on the pyridine-4-ol ring of B-ligand while the LUMO is on the pyridyl ring of B-ligand. The HOMO and LUMO energies of all the complexes (**1–3**) are tabulated in Table 3. It is seen that the major transitions for absorption are from HOMO to LUMO +1, where as for emission are from HOMO to LUMO (see details in Table S1). In the emission spectra similar to the absorption spectra, the HOMO, LUMO, and LUMO+1 energy levels of (**1–3**) are lower than that of *mer*-Alq3 and the energy gaps are found to be ~0.64–0.75 eV higher than the *mer*-Alq3 [45], which reflects in their emission spectra.

3.4 Absorption and emission spectra properties

Several investigations have shown that TDDFT is a good predictive tool for absorption spectra; hence, the TDDFT calculations have been carried out for all the complexes (**1–3**). Like the earlier reports on similar molecules to determine the functional having the best performance, various functionals namely SVWN, BLYP, B3LYP, B3PW91, and PBE0 are used to calculate the absorption λ_{max} values of **1** using the 6-31G(D) basis set (see details in Table S2)

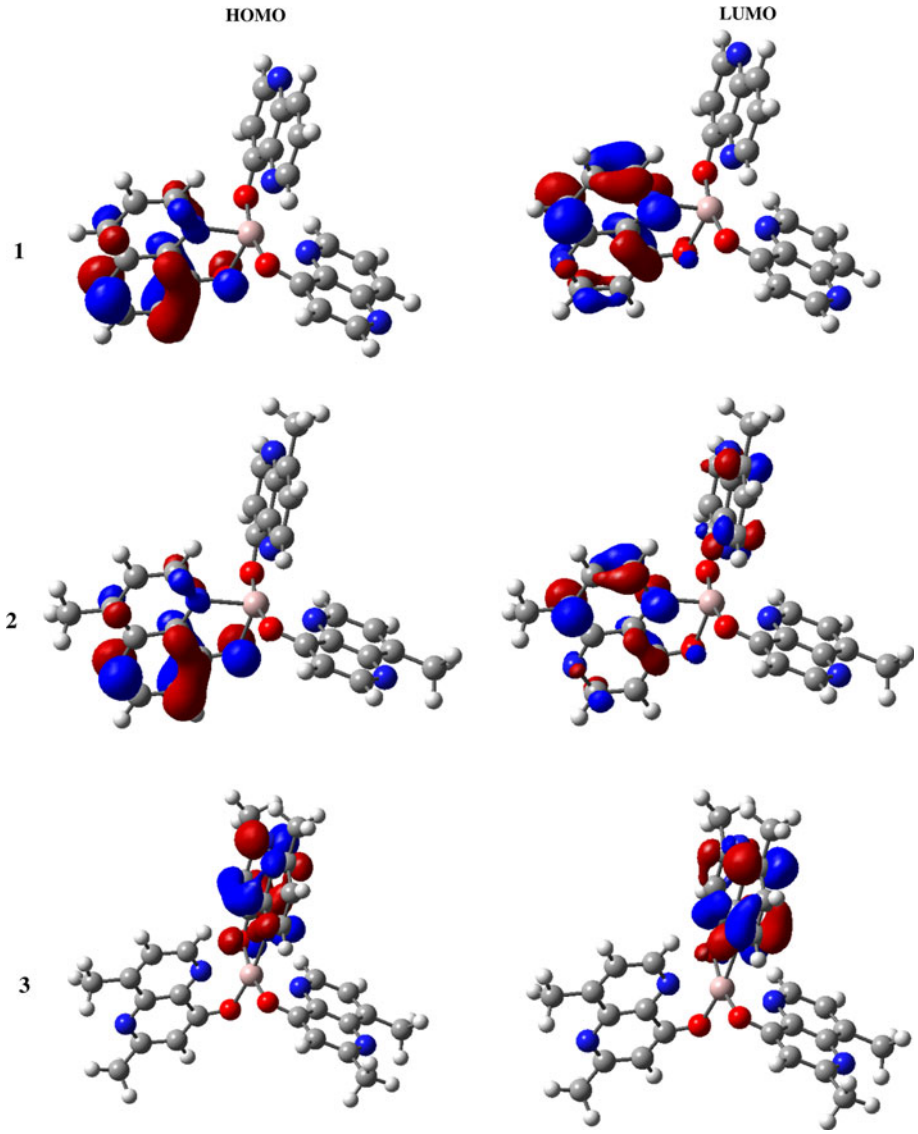

Fig. 3 Frontier molecular orbitals (FMOs) (0.05 e au^{-3}) for the excited states (S_1) of (**1–3**)

Table 3 HOMO, LUMO, and energy gaps (E_{gap}) of (**1**–**3**) (in eVs) in their excited state (S_1) obtained by using the TD-PBE0/6-31G(D)//CIS/6-31G(D) method

Complexes	HOMO	LUMO	E_{gap}
Alq3	−4.873	−1.649	3.224
1	−5.894	−2.032	3.862
2	−5.752	−1.792	3.960
3	−5.875	−1.902	3.973

[31, 32, 38]. It is seen that the calculations employing a variety of functional forms indicate that the absorption λ_{max} values vary significantly according to the employed functionals (Table S2). The performance of the local density approximation (SVWN) and pure gradient-corrected functionals (BLYP) is found to be poor. The results using the hybrid functionals (B3LYP, B3PW91, and PBE0) are much better. It can be seen that PBE0/6-31G(D) gives more reliable values than all other functionals (Table S2). Compared with the previously reported absorption of 367 and 366 nm using B3LYP/6-31G and B3LYP/3-21G(D) methods, respectively [29] for **1**, the absorption calculated using PBE0/6-31G(D) method, i.e., 350 nm is found to be in good agreement with the experiment [25]. To investigate the effect of the extension of the basis sets on the absorption spectra of **1**, calculations have been carried out using PBE0 method with 6-31+G(D), 6-31G, and 3-21+G(D) basis sets, and it is found that the basis set has negligible effect on the absorption (Table S2). Hence, PBE0 functional with 6-31G(D) basis set has been used further to calculate the absorption and emission spectra of all the complexes (**1**–**3**), and the results are summarized in Table 4 along with experimentally reported absorption and emission wavelengths [25]. It is seen from the Table 4, in all these complexes, the major transitions for absorption are from HOMO to LUMO+1 while for emission are from HOMO to LUMO. Due to the increase in the energy gaps (Tables 2, 3), the absorption and emission spectra of all the complexes are blue shifted compared with the *mer*-Alq3. It can be seen that the absorption spectra being blue shifted ~60–69 nm compared with the *mer*-Alq3 while the emission spectra being blue shifted ~121–141 nm. It can also be seen that the calculated absorption vales are in good agreement with the experimental values with deviations being 9, 4, and 6 nm for **1**, **2**, and **3**, respectively, while in case of the emission spectra the deviations being 31, 31, and 34 nm for **1**, **2**, and **3**, respectively.

3.5 Charge transfer integrals and reorganization energies

The band theory model [46, 47] and the hopping model [48–55] are widely used for describing the charge transport in organic materials. When the overlap of the molecular orbitals is strong, the bands are formed through which the conduction of the charge takes place according to the band theory model. On the other hand, the hopping model is more suitable where coupling between neighboring molecules is small. The latter model is more appropriate in our case here. In this model, the intermolecular charge transport is calculated by assuming that the charge hops between two molecules. The hole and electron transport processes at the molecular level in the electroluminescent layer can then be portrayed as the electron/hole transfer reactions between the neighboring molecules [55–65] as

$$A^{+/-} + A^0 \rightarrow A^0 + A^{+/-}, \quad (1)$$

where $\mathbf{A^{+/-}}$ indicates the molecule in a cationic or anionic state and $\mathbf{A^0}$ is a neighboring molecule in the neutral state. In case of electron transport, the interaction can be considered between a molecule in the neutral state and with a radical anion, and in the case of hole transport, the interaction can be considered between a molecule in the neutral state and a radical cation.

The charge transfer rate can be defined using the Marcus theory [56].

$$K_{et} = \left(4\pi^2/h\right)\tau^2(4\pi\lambda kT)^{-1/2}\exp(-\lambda/4kT) \quad (2)$$

Here, τ is the charge transfer integral/coupling matrix element between neighboring molecules, λ is the reorganization energy, k is the Boltzmann constant, and

Table 4 Calculated absorption (λ_{abs}) and emission (λ_{emi}) wavelengths (in nms) of (**1**–**3**) obtained by using the TD-PBE0/6-31G(D) method

Complex	Major transitions[a]	λ_{abs}	f[b]	Exp. λ^c_{abs}	Major transitions	λ_{emi}	f[b]	Exp. λ^c_{emi}
Alq3[d]	H → L+1	410	0.0759	387	H ← L	523	0.0441	515
1	H → L+1	350	0.1029	341	H ← L	402	0.073	433
2	H → L+1	342	0.1408	338	H ← L	384	0.111	415
3	H → L+1	341	0.1319	335	H ← L	382	0.103	416

[a] H, L, and L+1 stand for HOMO, LUMO, and LUMO+1

[b] f is oscillator strength

[c] Experimental λ_{abs} and λ_{emi} for (**1**–**3**) from [25]

[d] Experimental λ_{abs} and λ_{emi} for Alq3 from [45]

T the temperature. The two major parameters that determine self-exchange electron-transfer rates and ultimately the charge mobility are the following: (a) the charge transfer/electronic coupling τ between neighboring molecules, which should be maximum and (b) the reorganization energy (λ) which should be small for significant transport. An evaluation of τ would require the relative positions of the molecules in the solid state as it is related to the energetic splitting of the frontier orbitals of the interacting molecules. On the other hand, hole/electron transports are predicted from the electron (λ_{ele}) and hole (λ_{hole}) reorganization energies, respectively, and are in good agreement with the experimental observations [55–65]. The reorganization energies are calculated based on the model as shown in scheme 1, and this model have been applied with success in many earlier studies [55–65]. Here, λ_1 is the energy required for the reorganization of the neutral geometry to the cation geometry upon removal of an electron and λ_2 is the energy required to reorganize the obtained cation geometry back to a neutral state upon reaccepting an electron. The sum of these energies gives the total reorganization energy for the hole transport ($\lambda_{hole} = \lambda_1 + \lambda_2$) of the molecule when the charge is being transported. In a similar fashion, the reorganization energy of the neutral to anion (λ_3) and back (λ_4) should be useful in understanding the electron transport (($\lambda_{ele} = \lambda_3 + \lambda_4$).

The electron/hole reorganization energies for *mer*-Alq3 [59], fluorinated derivatives of *mer*-Alq3 [31], with electron donating/withdrawing groups substituted on the ligands of *mer*-Alq3 [32], 5- and 6-coordinated Al-complexes [66] and dinuclear Alq3-complex [67] has been reported at B3LYP/6-31G(D) level. Hence, here also the reorganization energy calculations have been carried out on (**1**–**3**) using the same methodology and compared with that of *mer*-Alq3 (Table 4). It can be seen from Table 4 that both the λ_{ele} and λ_{hole} values of (**1**–**3**) are lower than that of *mer*-Alq3. As the number of methyl group substitution

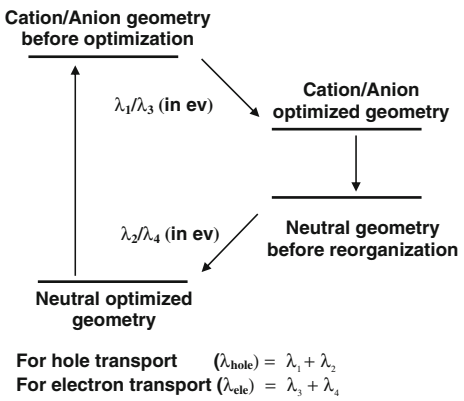

Scheme 1 Calculation of reorganization energy

(which acts as an activating group) increases, the λ_{ele} also increases, and the complex **3** has a value of 0.273 eV which is almost the same as of *mer*-Alq3. The calculated λ_{hole} (0.213 eV) and λ_{ele} (0.236 eV) values for AlND3(**1**) suggest that it has a lower reorganization energy than the electron transport. The charge transport integrals for hole (τ_{hole}) and electron (τ_{ele}) are calculated for AlND3(**1**) to get a more detailed picture of the electron/hole transport. For calculating these integrals, the relative positions of the two molecules in the hopping complexes are essential in an amorphous film, which can be considered approximately as a collection of molecules with relative positions similar to that in the crystalline state without long-range interactions. Here, we have chosen the crystal data for AlND3(**1**) [25] and simulated the relative positions of pairs of AlND3 molecules. As AlND3(**1**) belong to $P\bar{1}$ space group, and each unit cell has two molecules related by inversion symmetry. A charge on an AlND3 molecule can hop to others in the neighboring unit cells in two ways: the one related by translational symmetry as shown in pathways **I**–**III** (Fig. 4) and the other is related by inversion symmetry within the cell or by inversion symmetry as shown in pathways **IV**–**XI** (Fig. 4). The charge transfer integrals for Alq3 have been calculated by Lin et al. [59] using both the Koopmans theorem in conjugation with Hartree–Fock model (HF-KT) [68–73] and the direct coupling (DC) method implemented in Q-chem software [39–43]. Sometimes the HF-KT method fails due to the distorted HOMO and LUMO that are no longer simple linear combination of charge-localized orbitals [68–73]. Hence, the transfer integrals for **1** have been carried out using the DC-method (Table 5).

The charge transfer integrals for hole (τ_{hole}) and electron (τ_{ele}) between an AlND3 molecule and its neighbors are shown in Table 6, along with the Al–Al distance between hopping partners. It can be seen from the geometries of the hopping pairs (see details in supplementary Information), there exists two types of pathways namely the one in which the two ND ligand planes are parallel to each other (namely **IV** to **VII**, **X** and **XI**) and the other in which the two ND ligand planes deviates significantly from being parallel to each other (namely **I** to **III**, **VIII** and **IX**). The maximum overlap between the HOMOs and LUMOs of the two interacting molecules will result in a large value for the charge transfer integrals for the hole and electron. It can be seen from Table 6, when the Al–Al distance between the hopping pairs is large (pathways **II**–**V**), there is an inadequate overlap of two interacting orbitals resulting in smaller τ values. It can also be seen that the parallel pathways gives higher τ values when compared with the nonparallel pathways. This may be due to the large overlap of orbitals in the former. For e.g., the pathways namely **I**,

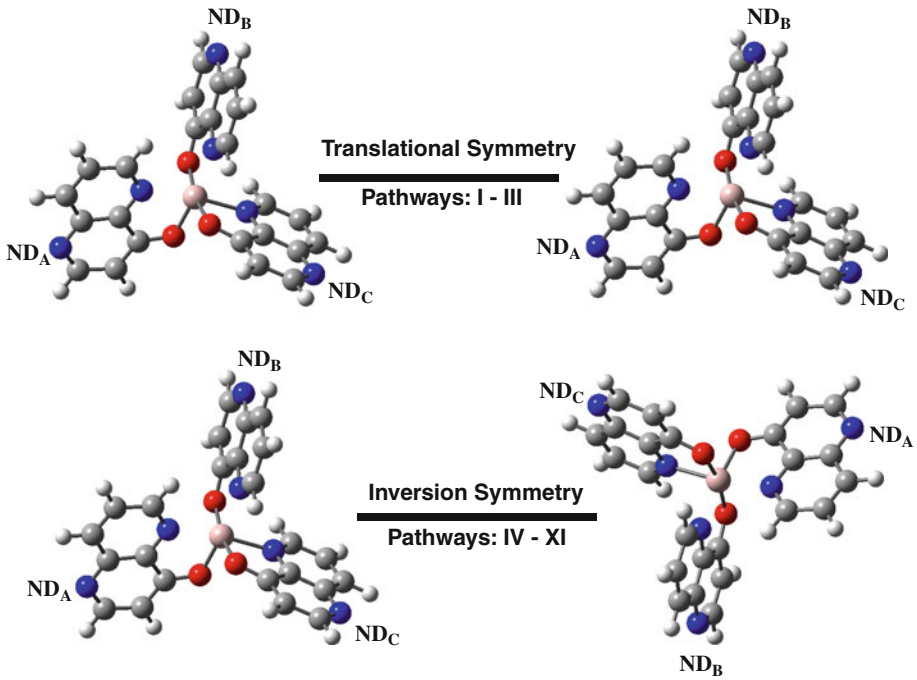

Fig. 4 All charge hopping pathways for a particular AlND3 molecule with another AlND3 molecule. (see supplementary information for the detailed pathways)

Table 5 Calculated reorganization energies (in eV) of (**1**–**3**) for hole (λ_{hole}) and electron (λ_{ele}) obtained by using the B3LYP/6-31G(D) method

Complexes	λ_{hole}	λ_{ele}
Alq3[a]	0.242	0.276
1	0.213	0.236
2	0.215	0.255
3	0.215	0.273

[a] Alq3 data from [59]

Table 6 Charge transfer integrals τ_{hole} for hole and τ_{ele} for electron between an AlND3(**1**) molecule and its neighbors using DC-method

Pathways	Al–Al distance (in Å)	$\tau_{hole}/10^{-4}$ (in eV)	$\tau_{ele}/10^{-4}$ (in eV)
I	7.995	8.61	41.67
II	12.088	4.51	2.23
III	13.115	0.77	0.06
IV	14.725	3.10E-05	9.40E-06
V	13.115	0.22	0.24
VI	9.406	128.19	70.35
VII	8.331	128.67	16.27
VIII	8.399	20.25	0.65
IX	8.349	5.36	1.78
X	8.156	78.56	107.52
XI	9.562	178.99	983.21

X and **XI** give higher τ_{ele} values, whereas the pathways namely **VI** and **VII** give higher τ_{hole} values compared with the nonparallel pathways. The lower τ values in other parallel pathways may be attributed to the cancellation of orbital overlap resulting in the poor overlap between the two interacting orbitals in the hopping pair. It can be seen from these results that the majority of the pathways are having higher τ_{ele} values when compared with the τ_{hole} suggests that AlND3(**1**) behaves as an electron transporter than hole transporter.

4 Conclusions

The ground-state (S_0) geometries of tris(4-hydroxy-1,5-naphthyridinato) aluminum (AlND3) and its methyl derivatives have been optimized at DFT/B3LYP/6-31G(D) method. From the frontier molecular orbitals, similar to mer-Alq3, it can be seen that in all these complexes, the HOMO is localized on the pyridine-4-ol ring of A-ligand while LUMO is on the pyridyl ring of B-ligand in the S_0 states irrespective of the methyl substitution present on the ligands. The CIS/6-31G(D) method have been used to obtain the first singlet excited (S_1) states. The absorption and emission spectra calculations are carried out at TD-PBE0/6-31G(D) level and are found to be comparable with the experimental data. A significant blue shift for all these complexes can be interpreted from the theoretical results. The reorganization energies for the hole/electron transport and charge transfer integrals have been calculated. The results show that AlND3 behaves as an electron transport material. Thus, the theoretical study of structural, electronic, and charge transport properties of such complexes may be useful in designing the high-performance emitting materials used in OLEDs.

Acknowledgments The authors thank the Director, IICT and the Head, Inorganic Chemistry division, IICT for their constant encouragement in this work.

References

1. Burroughes JH, Bradley DDC, Brown AR, Marks RN, Mackay K, Friend RH, Burns PL, Holmes AB (1990) Nature 347:539
2. Friend RH, Gymer RW, Holmes AB, Burroughes JH, Marks RN, Taliani C, Bradley DDC, Dos Santos DA, Bredas JL, Logdlund M, Salaneck WR (1999) Nature 397:121
3. Mitsche U, Bauerle P (2000) J Mater Chem 10:1471
4. Chen CH, Shi J (1998) Coord Chem Rev 171:161
5. Tang CW, VanSlyke SA (1987) Appl Phys Lett 51:913
6. Tang CW, VanSlyke SA, Chen CH (1989) J Appl Phys 65:3610
7. Hamada Y (1997) IEEE Trans Electron Devices 44:1208
8. Chen CH, Shi J (1998) Coord Chem Rev 171:161
9. VanSlyke SA, Chen CH, Tang CW (1996) Appl Phys Lett 69:2160
10. Curioni A, Boero M, Andreoni W (1998) Chem Phys Lett 294:263
11. Curioni A, Andreoni W (1999) J Am Chem Soc 121:8216
12. Curioni A, Andreoni W, Treusch R, Himpsel RF, Haskal E, Seidler P, Kakar S, van Buuren T, Terminello L (1998) J Appl Phys Lett 72:1575
13. Johansson N, Osada T, Stafstrom S, Salaneck WR, Parente V, dos Santos DA, Crispin X, Bredas JL (1999) J Chem Phys 111:2157
14. Halls MD, Aroca R (1998) Can J Chem 76:1730
15. Kushto GP, Iizumi Y, Kido J, Kafafi ZH (2000) J Phys Chem A 104:3670
16. Amati M, Lelj F (2002) Chem Phys Lett 363:451
17. Burrows PE, Shen Z, McCarty DM, Forrest SR, Cronin JA, Thompson ME (1996) J Appl Phys 79:7991
18. Su Z, Cheng H, Gao H, Sun S, Chu B, Wang R, Wang Y (2000) Gaodeng Xuexiao Huaxue Xuebao 211:416
19. Anderson S, Weaver MS, Hudson AJ (2000) Synth Met 111:459
20. Martin RL, Kress JD, Campbell IH, Smith DL (2000) Phys Rev B 61:15804
21. Stampor W, Kalinowski J, Marconi G, Di Marco P, Fattori V, Giro G (1998) Chem Phys Lett 283:373
22. Bacon AD, Zerner MC (1979) Theor Chim Acta 53:21
23. Zhang RQ, Lee CS, Lee ST (2000) Chem Phys Lett 326:413
24. Sugimoto M, Sakaki S, Sakanoue K, Newton MD (2001) J Appl Phys 90:6092
25. Liao SH, Shiu JR, Liu SW, Yeh SJ, Chen YH, Chen CT, Chow TJ, Wu CI (2009) J Am Chem Soc 131:763
26. Frisch MJ, Trucks GW, Schlegel HB, Scuseria GE, Robb MA, Cheeseman JR, Montgomery JA Jr, Vreven T, Kudin KN, Burant JC, Millam JM, Iyengar SS, Tomasi J, Barone V, Mennucci B, Cossi M, Scalmani G, Rega N, Petersson GA, Nakatsuji H, Hada M, Ehara M, Toyota K, Fukuda R, Hasegawa J, Ishida M, Nakajima T, Honda Y, Kitao O, Nakai H, Klene M, Li X, Knox JE, Hratchian HP, Cross JB, Bakken V, Adamo C, Jaramillo J, Gomperts R, Stratmann RE, Yazyev O, Austin AJ, Cammi R, Pomelli C, Ochterski JW, Ayala PY, Morokuma K, Voth GA, Salvador P, Dannenberg JJ, Zakrzewski VG, Dapprich S, Daniels AD, Strain MC, Farkas O, Malick DK, Rabuck AD, Raghavachari K, Foresman, JB, Ortiz JV, Cui Q, Baboul AG, Clifford S, Cioslowski J, Stefanov BB, Liu G, Liashenko A, Piskorz P, Komaromi I, Martin RL, Fox DJ, Keith T, Al-Laham MA, Peng CY, Nanayakkara A, Challacombe M, Gill PMW, Johnson B, Chen W, Wong MW, Gonzalez C, Pople JA (2001) Gaussian 03, Revision D.01. Gaussian Inc, Wallingford
27. Zhang J, Frenking G (2004) J Phys Chem A 108:10296
28. Zhang J, Frenking G (2004) Chem Phys Lett 394:120
29. Gahungu G, Zhang J (2005) J Phys Chem B 109:17762
30. Irfan A, Cui R, Zhang J (2008) J Mol Struct THEOCHEM 850:79
31. Irfan A, Cui R, Zhang J (2009) Theor Chem Acc 122:275
32. Irfan A, Zhang J (2009) Theor Chem Acc 124:339
33. Halls MD, Schlegel HB (2001) Chem Mater 13:2632
34. Gahungu G, Zhang J (2005) Chem Phys Lett 410:302
35. Yang Z, Yang S, Zhang J (2007) J Phys Chem A 111:6354
36. Hu B, Gahungu G, Zhang J (2007) J Phys Chem A 111:4965
37. Sun M, Niu B, Zhang J (2008) J Mol Struct THEOCHEM 862:85
38. Teng YL, Kan YH, Su ZM, Liao Y, Yang SY, Wang RS (2007) Theor Chem Acc 117:1
39. You ZQ, Shao Y, Hsu CP (2004) Chem Phys Lett 390:116
40. Farazdel A, Dupuis M, Clementi E, Aviram A (1990) J Am Chem Soc 112:4206
41. King HF, Stanton RE, Kim H, Wyatt RE, Parr RG (1967) J Chem Phys 47:1936
42. Zhang LY, Friesner RA, Murphy RB (1997) J Chem Phys 107:450
43. Shao Y, Molnar LF, Jung Y, Kussmann J, Ochsenfeld C, Brown ST, Gilbert ATB, Slipchenko LV, Levchenko SV, O'Neill DP, DiStasio RA Jr, Lochan RC, Wang T, Beran GJO, Besley NA, Herbert JM, Lin CY, Voorhis TV, Chien SH, Sodt A, Steele RP, Rassolov VA, Maslen PE, Korambath PP, Adamson RD, Austin B, Baker J, Byrd EFC, Dachsel H, Doerksen RJ, Dreuw A, Dunietz BD, Dutoi AD, Furlani TR, Gwaltney SR, Heyden A, Hirata S, Hsu CP, Kedziora G, Khalliulin RZ, Klunzinger P, Lee AM, Lee MS, Liang W, Lotan I, Nair N, Peters B, Proynov EI, Pieniazek PA, Rhee YM, Ritchie J, Rosta E, Sherrill CD, Simmonett AC, Subotnik JE, Woodcock HL III, Zhang W, Bell AT, Chakraborty AK, Chipman DM, Keil FJ, Warshel A, Hehre WJ, Schaefer HF III, Kong J, Krylov AI, Gill PMW, Gordon MH (2006) Phys Chem Chem Phys 8:3172
44. Jonas V, Frenking G, Reetz MT (1994) J Am Chem Soc 116:8741
45. Shi YW, Shi MM, Huang JC, Chen HZ, Wang M, Liu XD, Ma YG, Xu H, Yang B (2006) Chem Commun 18:1941
46. Bredas JL, Calbert JP, da Silva Filho DA, Cornil J (2002) Proc Natl Acad Sci USA 99:5804
47. Cheng YC, Silbey RJ, da Silva Filho DA, Calbert JP, Cormil J, Bredas JL (2003) Chem Phys 118:3764
48. Marcus RA, Sutin N (1985) Biochim Biophys Acta 811:265
49. Barbara PF, Meyer TJ, Ratner MA (1996) J Phys Chem 100:13148
50. Sakanoue K, Motoda M, Sugimoto M, Sakaki S (1999) J Phys Chem A 103:5551
51. Malagoli M, Bredas JL (2000) Chem Phys Lett 327:13
52. Li XY, Tong J, He FC (2000) Chem Phys 260:283
53. Nelsen SF, Trieber DA II, Ismagilov RF, Teki Y (2001) J Am Chem Soc 123:5684
54. Nelsen SF, Blomgren FJ (2001) Org Chem 66:6551
55. Lin BC, Cheng CP, Lao ZPM (2003) J Phys Chem A 107:5241
56. Marcus RA (1956) J Chem Phys 24:966
57. Cornil J, Lemaur V, Calbert JP, Bredas JL (2002) Adv Mater 14:726
58. Deng WQ, Goddard WA III (2004) J Phys Chem B 108:8614
59. Lin BC, Cheng CP, You ZQ, Hsu CP (2005) J Am Chem Soc 127:66
60. Curioni A, Boero M, Andreoni W (1998) Chem Phys Lett 294:263
61. Wang I, Estelle BA, Olivier S, Alain I, Baldeck PL (2002) J Opt A Pure Appl Opt 4:S258
62. Bredas JL, Beljonne D, Coropceanu V, Cornil J (2004) Chem Rev 104:4971
63. Raghunath P, Reddy AM, Gouri C, Bhanuprakash K, Rao VJ (2006) J Phys Chem A 110:1152

64. Yang L, Feng JK, Ren AM (2007) J Mol Struct: THEOCHEM 816:161
65. Liu YL, Feng JK, Ren AM (2007) J Phys Org Chem 20:600
66. Wang W, Dong S, Yin S, Yang J, Lu J (2008) J Mol Struct: Theochem 867:116
67. Fang XH, Hao YY, Han PD, Xu BS (2009) J Mol Struct: Theochem 896:44
68. Jordan KD, Paddon Row MN (1992) J Phys Chem 96:1188
69. Liang C, Newton MD (1992) J Phys Chem 96:2855
70. Curtiss LA, Naleway CA, Miller JR (1993) J Phys Chem 97:4050
71. Rodriguez ML, Larsson S (1997) Int J Quantum Chem 61:847
72. Li XY, Tang XS, He FC (1999) Chem Phys 248:137
73. Lu SZ, Li XY, Liu JF (2004) J Phys Chem A 108:4125